Novel Metabolomic Profile of Subjects with Non-classic Apparent Mineralocorticoid Excess

Alejandra Tapia-Castillo
Pontificia Universidad Católica de Chile
Cristian Carvajal
Pontificia Universidad Católica de Chile
Andrea Vecchiola
Pontificia Universidad Católica de Chile
Carlos Fardella (cfardella@med.puc.cl)
Pontificia Universidad Católica de Chile

Research Article

Keywords: metabolomics, nonclassic AME, mineralocorticoid receptor, hypertension

Posted Date: December 7th, 2020

DOI: https://doi.org/10.21203/rs.3.rs-117407/v1

Abstract

Nonclassic apparent mineralocorticoid excess (NC-AME) is proposed as a novel clinical condition with a mild phenotypic spectrum that ranges from normotension to severe hypertension. This condition is mainly characterized by a high serum cortisol to cortisone ratio (F/E) and concomitant low cortisone (E), however further metabolic changes in NC-AME have not been studied. A cross-sectional study was performed in a primary-care cohort of 396 Chilean subjects, which were classified in two groups: NC-AME (n=28) and healthy controls (n=27). An untargeted metabolomics assay in serum samples from both groups was performed by UPLC-Q-TOF/MS. Global metabolic variations were assayed by principal component analysis (PCA) and further compared by orthogonal partial least-squares discriminant analysis (OPLS-DA). NC-AME subjects exhibited higher values of blood pressure, fractional excretion of potassium, and lower plasma renin activity and urinary sodium to potassium ratio. Metabolomic analyses showed 36 differentially regulated metabolites between NC-AME and control subjects. The ROC curve analyses identified eight metabolites with high discriminatory capacity between NC-AME and control subjects. Moreover, gamma-L-glutamyl-L-methionine sulfoxide and 5-sulfoxymethylfurfural (SMF), exhibited significant association with cortisone, which are potential biomarkers of NCAME, however further assays should elucidate its biological role in setup and progression of this phenotype.

Introduction

Apparent mineralocorticoid excess (AME) syndrome is an infrequently occurring autosomal recessive disorder caused by mutations in coding regions of the HSD11B2 gene [1], and AME is characterized by the activation of the mineralocorticoid receptor (MR) by cortisol. It is known that cortisol can bind to MR with equal affinity to aldosterone, leading to the same effects as primary aldosteronism (PA) [2,3]. However, under normal conditions, activation of the MR by cortisol does not occur because the 11β-hydroxysteroid dehydrogenase type 2 (11β-HSD2) enzyme inactivates cortisol in cortisone and thus prevents cortisol from binding to the MR [4]. In the literature, there is clear evidence demonstrating that a total deficit of 11β-HSD2 triggers severe arterial hypertension that is characterized by a childhood onset and is associated with suppressed plasma renin activity (PRA), low aldosterone levels and hypokalemic alkalosis [5-8].

Recent studies by our group identified mild forms of AME syndrome that we named nonclassic apparent mineralocorticoid excess (NC-AME), which is proposed to be a condition with a wider and milder phenotypical spectrum than was identified for AME [5,7,9-12] and is primarily characterized by a high F/E ratio and low cortisone [9]. In addition, NC-AME patients have higher levels of inflammatory markers, such as microalbuminuria and plasminogen activator inhibitor-1 (PAI-1), and they have high sensitivity c reactive protein (hs-CRP). To date, the cause of NC-AME has not been elucidated. However, we recently determined that NC-AME could be associated with minor genetic defects (i.e., heterozygous pathogenic variant or polymorphisms) [9] or epigenetic modifications such as miRNAs [13]. However, salt intake, glycyrrhetinic acid-like factors (GALFs) and environmental factors [5] have been hypothesized to be factors that deregulate the expression and activity of HSD11B2.

Previous studies described the presence of inhibitor substances of the 11β-HSD2 enzyme in human urine, which could include GALFs, such as the licorice derivative glycyrrhetinic acid (GA), which inhibits the metabolism of glucocorticoids [14]. A large proportion of patients with essential hypertension likely exhibit endogenous GALF-like inhibitors [14], particularly endogenous allo-3α-5α-reduced pathway steroidal products, corticosterone and 11-dehydrocorticosterone [15], derivatives of progesterone and adrenocorticosteroids [16,17], 11β-OH-testosterone and 11-keto-testosterone, which are potent inhibitors of 11β-HSD2 dehydrogenase activity. Moreover, several publications have showed the effects of inhibition of 11β-HSD2 by others environmental inhibitors, including licorice, GA, carbenoxolone and others previously described [17-20].

Metabolomics can be employed to detect global metabolite profiles [21], which represent the endpoint of all metabolic activities and help to characterize various biological and physiological processes. Previous studies of untargeted metabolomics in resistant hypertension have shown changes in metabolite levels related to fatty acid, lipid, amino acid and purine metabolism [22], showing that metabolomics helps to elucidate the metabolites that may influence the physiopathology associated with drug-resistant hypertension.

In the present study, we attempted to identify metabolite profiles in NC-AME subjects by employing an untargeted metabolomic approach to elucidate impaired pathways and obtain insights into the biological mechanisms underlying NC-AME, and we attempted to identify novel biomarkers associated with this phenotype.

Subjects And Methods

Subjects

This study is designed as a cross-sectional study in a Chilean adult cohort of 396 subjects aged 18 to 60 years and of both genders with a similar socioeconomic status and ethnicity; these subjects had been previously recruited from primary care centers in Santiago, Chile. The study was performed according to the principles of the Declaration of Helsinki. A written informed consent was signed by all participants. Consent and ethics approval for the recruitment of patients and samples is included in the certificate of approval CEC-MEDUC 14-268 (FONDECYT 1150437) and CEC-MEDUC 12-207 (FONDECYT 1130427), approved by the local ethics committee of the Faculty of Medicine, Pontificia Universidad Católica de Chile.

The subjects enrolled in this study meet the following criteria: absence of a history of chronic pathologies, such as renal failure, heart failure, diabetes mellitus, chronic liver damage, and endocrinopathies, and drugs affecting the PRA and aldosterone to PRA ratio (ARR) [23,24]. Subjects who received glucocorticoids (e.g., cortisol and prednisone) or mineralocorticoids (fludrocortisone) less than 2 months before the start of the study were also excluded, since both affect the aldosterone, PRA or urinary free cortisol (F) levels.

Clinical characteristics and biochemical assay

All subjects in this study had a clinical record and physical examination that included age, height, weight, body mass index (BMI) and blood pressure (BP) [13]. BP measurements were obtained from the right arm at consecutive 5-minute intervals using an oscillometric method (Dinamap CARESCAPE V100, GE Healthcare, Medical Systems Information Technologies, Milwaukee, WI), with the subjects remaining in a seated position. Hypertension-AHA guidelines were followed to identify blood pressure categories in our cohort [25].

After overnight fasting, basal blood samples were obtained between 08:00 and 10:00 AM. A biochemical profile was performed, including measurements of urine and plasma creatinine, electrolytes (sodium and potassium), aldosterone and PRA. Serum aldosterone and PRA were measured by radioimmunoassay using a commercial kit (Coat-A-Count Kit; Siemens, Los Angeles, CA and DiaSorin, Stillwater, MN, respectively). Serum cortisol and cortisone were quantified using liquid chromatography associated with tandem mass spectrometry (LC-MS/MS) and were validated according to the parameters suggested by the FDA and the CLSI using deuterated internal F and E standards (cortisol -d4 and cortisone-d2) in an Agilent 1200 Series HPLC unit coupled to an ABSciex 4500 QTrap mass spectrometer. All plasma, serum and urine (spot and 24-hour collection) samples were used immediately or were stored at -80°C.

After the exclusion criteria were applied, we studied 28 NC-AME subjects (7.1%), who were identified according to previously described parameters [9]. Briefly, NC-AME subjects have a low level of serum cortisone (E) ($E \leq 2.1$ μg/dl) and a high cortisol to cortisone (F/E) ratio ($F/E \geq 4.43$) [9]. The NC-AME subjects were compared with a control group of 27 normotensive subjects with BMI values less than 35, no clinical risk factors and no evident diagnosis of genetic diseases or secondary diseases.

Methods

Sample preparation for metabolic assays by LC-MS

A volume of 100 μl of serum sample was thawed and extracted with 300 μL of methanol and 5 μL of DL-o-chlorophenylalanine (2.8 mg/mL) (IS) with 30 seconds of vortexing. Then, all samples were kept at -40°C for 1 h. After that step, samples were vortexed for 30 seconds and centrifuged at 12000 rpm and 4°C for 15 min. Finally, 200 μL of supernatant was transferred to a vial for LC-MS analysis. Quality control (QC) samples were used to evaluate the methodology. The same amount of extract was obtained from each sample and mixed as QC samples. The QC samples were prepared using the same sample preparation procedure [26].

Untargeted metabolomics by UPLC-TOF-MS

Separation was performed by liquid chromatography in an Ultimate 3000LC combined with Q Exactive MS (Thermo) and screened with ESI-MS (targeted MS/MS mode). The LC system is composed of a Thermo Hyper gold C18 (100×2.1 mm 1.9 μm) with an Ultimate 3000LC. The mobile phase is composed of solvent A (0.1% formic acid-5% acetonitrile-water) and solvent B (0.1% formic acid-acetonitrile) with a gradient elution (0-1.5 min, 100-80% A; 1.5-9.5 min, 80-0% A; 9.5-14.5 min, 0% A; 14.5-14.6 min, 0-100% A; and 14.6-18 min, 100% A) [27]. The flow rate of the mobile phase was 0.3 $mL \cdot min^{-1}$. The column temperature was 40°C, and the sample manager temperature was set at 4°C [26]. The mass spectrometry parameters in ESI+ and ESI- mode are listed as follows: ESI+: Heater Temp 300°C; Sheath Gas Flow rate, 45 arb; Aux Gas Flow Rate, 15 arb; Sweep Gas Flow Rate, 1 arb; spray voltage, 3.0 kV; Capillary Temp, 350°C; S-Lens RF Level, 30%. ESI-: Heater Temp 300°C, Sheath Gas Flow rate, 45 arb; Aux Gas Flow Rate, 15 arb; Sweep Gas Flow Rate, 1 arb; spray voltage, 3.2 kV; Capillary Temp, 350°C; and S-Lens RF Level, 60% [26,27].

At the beginning of the sequence, we run four QC samples to avoid small changes in both chromatographic retention time and signal intensity. The QC samples are also injected at regular intervals (every ten samples) throughout the analytical run.

Data and statistical analysis

The raw data are acquired and aligned using Compound Discover (3.0, Thermo) based on the m/z value and the retention time of the ion signals. Ions from both ESI- and ESI+ were merged and imported into the SIMCA-P program (version 14.1) to enable multivariate analysis. Principal component analysis (PCA) is first used as an unsupervised method for data visualization and outlier identification. Supervised regression modeling is then performed on the data set by use of partial least squares discriminant analysis (PLS-DA) or orthogonal partial least squares discriminant analysis (OPLS-DA) to identify the potential metabolites that may serve as biomarkers. The potential metabolites were filtered and confirmed by combining the results of the variable importance in projection (VIP) values (VIP > 1.0) and t-

tests ($p < 0.05$) [27]. The quality of the fitting model can be explained by R2 and Q2 values. R2 displays the variance in the model and indicates the quality of the fit. Q2 displays the variance in the data, indicating the model's predictability [28].

Pathway analysis was performed based on the KEGG and MBRole databases. All significant metabolites were imported to obtain categorical annotations, including pathways, enzyme interactions and other biological annotations.

To define the clinical significance and certify the robustness of the mathematical scoring-based classification employed to distinguish between NC-AME and control subjects, receiver operating characteristic (ROC) curve analysis was performed. The relationship between serum cortisone values and metabolomics-derived variables was also assessed individually using linear regression analysis. All analyses were performed using SPSS 20 and GraphPad Prism v5.0 software.

Results

Clinical and biochemical profile of NC-AME subjects

The baseline characteristics of both 28 NC-AME subjects and 27 healthy controls are shown in Table 1. NC-AME subjects had significantly higher values of SBP ($p < 0.0001$), DBP ($p < 0.0001$), fractional excretion of potassium (FEK) ($p = 0.03$) and serum F/E ($p = 0.01$) and a lower PRA ($p = 0.005$), serum cortisone ($p <0.0001$) and urinary Na/K ratio ($p = 0.004$). Both groups exhibited comparable serum aldosterone and cortisol levels (Table 1).

Table 1
Clinical and biochemical characteristics of the studied subjects

	NC-AME	Controls	P value
N	28	27	—
Male, n (%)	11 (39.3%)	12 (44.4%)	0.6
Age (years)	51.1 [37.7 - 58.0]	40.7 [33.2 - 49.8]	0.14
BMI (kg/m2)	27.7 [26.1 - 30.1]	26.5 [24.6 - 28.9]	0.13
SBP (mm Hg)	141.0 [120.0 - 154.2]	115.7 [108.7 - 119.0]	<0.0001*
DBP (mm Hg)	88.5 [78.7 - 97.5]	74.7 [70.0 - 75.7]	<0.0001*
Serum cortisol (ug/dl)	9.9 [8.6 - 12.5]	10.4 [7.4 - 16.7]	0.8
(nmol/L)	273.1 [237.2 – 344.8]	286.9 [204.1 – 460.7]	
Serum cortisone (ug/dl)	1.9 [1.8 - 2.1]	2.4 [2.1 - 2.8]	<0.0001*
(nmol/L)	52.7 [49.9 – 58.3]	66.6 [58.3 – 77.7]	
Serum F/E ratio	5.3 [4.7 - 6.1]	4.4 [3.7 - 5.9]	0.01*
PRA (ng/ml*h)	1.0 [0.7 - 1.8]	1.5 [1.3 - 2.0]	0.005*
(ng/L/s)	0.3 [0.2 – 0.5]	0.4 [0.4 – 0.6]	
Aldosterone (ng/dl)	8.9 [5.4 - 13.6]	7.5 [5.6 - 11.7]	0.3
(pmol/L)	246.9 [149.8 – 377.4]	208.1 [155.4 – 324.6]	
Serum Na (mEq/L)	141 [139 - 143]	140 [139 - 141]	0.2
Serum K (mEq/L)	4.1 [3.9 - 4.4]	4.3 [4.0 - 4.4]	0.4
FeNa (24h %)	0.6 [0.4 - 0.8]	0.7 [0.6 - 0.9]	0.1
FEK (24h %)	8.4 [6.3 - 10.7]	6.7 [5.7 - 8.3]	0.03*
Urinary Na (mEq/24h)	124 [86 - 173]	141 [110 - 194]	0.2
Urinary K (mEq/24h)	49.5 [38.0 - 62.8]	45.0 [27.0 - 59.0]	0.2
Urinary Na/K	2.4 [1.6 - 3.5]	3.5 [2.4 - 4.2]	0.004*

Values correspond to median [Q1-Q3]. *p< 0.05, Mann–Whitney test. BMI, body mass index; SBP, systolic blood pressure; DBP, diastolic blood pressure; F/E, cortisol to cortisone ratio; PRA, plasma renin activity; Na, sodium; K+, potassium; FENa, fractional excretion of sodium; FEK, fractional excretion of potassium.

Plasma metabolomic profiling

To identify metabolite changes in NC-AME, we acquired untargeted metabolomic profiling of all serum samples in the discovery setup based on UPLC-Q-TOF/MS in both positive and negative ion modes. The data were obtained with the mass-to-charge ratio (m/z), retention time (RT) and data matrix of the peak area. In the positive and negative ion modes, we obtained 2798 and 3503 metabolites, respectively. The ion features of the QC samples were employed to calculate the relative standard deviation (RSD) (Supplemental Figure 1A and 1B). The percentage of RSD distribution was less

than 30 (Supplemental Figure 2A and 2B). Thus, all of these findings indicated that the metabolomics analysis exhibited good reproducibility in this study (Supplemental Figure 3A and 3B).

To investigate the global metabolic variations, we first used PCA to analyze all samples acquired in both ion modes. The PCA plot (Supplemental Figure 4A and 4B) presents an overview of all samples in the data and exhibits an unclear grouping trend between both groups (NC-AME and controls). Thus, to eliminate any nonspecific effects of the operative technique and to confirm the metabolites, PLS-DA or OPLS-DA was performed to compare metabolic changes and characterize the differences between the NC-AME and control groups, respectively. As expected, the PLS-DA score plot (Supplemental Figure 5) or the OPLS-DA score plot (Figure 1) showed a clear separation of the control versus the NC-AME groups. Afterwards, the significantly changed metabolites (ions) between the groups were filtered out based on the variable importance of the projection values (VIP > 1.0) (Supplemental Figure 6A/6B and 7A/7B).

The significantly differential metabolites of the NC-AME patients compared with the control subjects were visualized through volcano plots (Figure 2). The results showed that 21 (in the negative ion model) (Table 2) and 15 (in the positive ion model) (Table 3) differential metabolites distinguished the NC-AME patients from the healthy controls. Among these 36 metabolites from the NC-AME patients, three metabolites were significantly upregulated, and thirty-three were downregulated (Table 2 and Table 3), compared with the respective metabolites from healthy controls. The heat plot of the differential metabolites in NC-AME versus control subjects is presented in Figure 3, in which color intensity correlates with the degree of increase (red) and decrease (green) relative to the mean metabolite ratio.

Table 2
Identified metabolites in negative ion model related to NC-AME based on UPLC-Q-TOF/MS.

Negative ion model						
Retention time [min]	**Molecular Weight (g/mol)**	**Compound name**	**Formula**	**Pathway**	**Fold Change**	**P value**
2,664	193,040	L-Dopachrome	C9H7NO4	Tyrosine Metabolism	2,754	0,000
1,706	294,088	gamma-L-Glutamyl-L-methionine sulfoxide	C10H18N2O6S	-	2,162	0,000
4,798	192,026	Citric acid	C6H8O7	Transfer of Acetyl Groups into Mitochondria Citric Acid Cycle Warburg Effect	0,357	0,000
0,901	214,024	Deoxyribose 1-phosphate	C5H11O7P	Pentose Phosphate Pathway Pyrimidine Metabolism Purine Metabolism	0,475	0,000
0,898	178,047	L-Gulonolactone	C6H10O6	-	0,447	0,001
3,014	904,475	CL(8:0/8:0/8:0/8:0)	C41H78O17P2	-	0,381	0,001
4,045	584,263	Bilirubin	C33H36N4O6	Porphyrin Metabolism	0,387	0,002
0,942	296,071	Gyrocyanin	C17H12O5	-	0,018	0,006
0,923	246,050	Glycerophosphoglycerol	C6H15O8P	-	0,111	0,014
0,935	244,034	Fucose 1-phosphate	C6H13O8P	Fructose and Mannose Degradation	0,362	0,016
0,891	182,078	Mannitol	C6H14O6	-	0,002	0,015
2,212	205,987	5-Sulfoxymethylfurfural	C6H6O6S	-	2,868	0,027
4,282	496,230	Glaucarubin	C25H36O10	-	0,135	0,017
11,369	540,438	TG(i-13:0/8:0/8:0)	C32H60O6	-	0,585	0,004
3,891	244,003	(2E)-3-[3-(sulfooxy)phenyl]prop-2-enoic acid	C9H8O6S	-	0,390	0,014
3,634	490,311	1-(13Z,16Z-docosadienoyl)-glycero-3-phosphate	C25H47O7P	-	0,017	0,022
12,411	596,501	TG(8:0/13:0/12:0)	C36H68O6	-	0,595	0,010
11,866	442,402	MG(24:0/0:0/0:0)	C27H54O4	-	0,544	0,010
3,138	372,105	Dihydroferulic acid 4-O-glucuronide	C16H20O10	-	0,442	0,036
3,65	428,310	Glyceryl lactooleate	C24H44O6	-	0,073	0,036

4,486	286,189	Androstenedione	C19H26O2	Androstenedione Metabolism Androgen and Estrogen Metabolism	0,011	0,036

Table 3
Identified metabolites in positive ion model related to NC-AME based on UPLC-Q-TOF/MS.

Positive ion model						
Retention time [min]	**Molecular Weight (g/mol)**	**Compound name**	**Formula**	**Pathway**	**Fold Change**	**P value**
4,047	584,265	Bilirubin	C33H36N4O6	Porphyrin Metabolism	0,339	0,000
3,011	904,478	CL(8:0/8:0/8:0/8:0)	C41H78O17P2	-	0,417	0,001
2,822	239,062	S-Phenylmercapturic acid	C11H13NO3S	-	0,346	0,005
1,292	85,053	2-Pyrrolidinone	C4H7NO	-	0,086	0,012
5,989	308,184	(R)-1-O-b-D-glucopyranosyl-1,3-octanediol	C14H28O7	-	0,061	0,012
0,883	384,125	S-Adenosylhomocysteine	C14H20N6O5S	Methionine Metabolism Histidine Metabolism Glycine and Serine Metabolism Tryptophan Metabolism Tyrosine Metabolism Arginine and Proline Metabolism Methylhistidine Metabolism Betaine Metabolism Carnitine Synthesis Nicotinate and Nicotinamide Metabolism Estrone Metabolism Phosphatidylcholine Biosynthesis Catecholamine Biosynthesis Ubiquinone Biosynthesis	0,095	0,013
2,833	430,123	Ketoprofen glucuronide	C22H22O9	-	0,151	0,013
0,905	232,056	(2E,11Z)-5-[5-(Methylthio)-4-penten-2-ynyl]-2-furanacrolein	C13H12O2S	-	0,096	0,015
1,018	192,090	Oxoamide	C10H12N2O2	-	0,361	0,016
0,901	165,077	L-Phenylalanine	C9H11NO2	Phenylalanine and Tyrosine Metabolism	0,426	0,021
5,988	132,079	6-Hydroxyhexanoic acid	C6H12O3	-	0,152	0,024
3,629	426,296	Leupeptin	C20H38N6O4	-	0,007	0,025
12,241	578,491	DG(15:0/18:2(9Z,12Z)/0:0)	C36H66O5	-	0,391	0,027

0,9	182,079	L-Iditol	C6H14O6	-	0,003	0,028
4,48	406,190	Carvedilol	C24H26N2O4	-	0,140	0,045

Enrichment and clustering of metabolites of interest

To identify the relationships of the metabolites, we constructed a correlation network diagram based on the KEGG databases and MBRole. Under the limiting condition of $P < 0.05$ in the MBRole, there are primarily 25 enriched metabolic pathways, including 36 highlighted metabolites, that were involved, while the methylhistidine metabolism and transfer of acetyl groups into mitochondria pathway ranked highest, which provides key information for constructing a metabolomic network diagram (Supplemental Figure 8A/8B).

Prediction regression model

To assess the diagnostic capacity of the significant metabolites in the identification of the NC-AME phenotype, we applied ROC curve analysis to the data. The area under the ROC curve for the upregulated metabolites, that is, L-dopachrome, gamma-L-glutamyl-L-methionine sulfoxide and 5-sulfoxymethylfurfural (SMF), was 0.95 (95% CI: 0.89-1.0), 0.78 (95% CI: 0.67-0.9), 0.67 (95% CI:0.53-0.8) respectively, in NC-AME subjects (Figure 4.A). The area under the ROC curve for downregulated metabolites, S-phenylmercapturic acid (SPMA), bilirubin, L-iditol, deoxyribose 1-phosphate, and citric acid, was 0.9 (95% CI: 0.82-0.97), 0.86 (95% CI: 0.77-0.95), 0.85 (95% CI: 0.75 - 0.94), 0.82 (95% CI: 0.71-0.93), and 0.78 (95% CI: 0.67-0.89) in NC-AME subjects, respectively (Figure 4.B).

Since low serum cortisone has been reported to be one of the best predictors of MR activation in NC-AME subjects [9], we performed regression analyses between serum cortisone and significant metabolites. Based on a linear regression analysis adjusted for age, BMI, SBP and DBP we identified a negative association of cortisone with gamma-L-glutamyl-L-methionine sulfoxide ($r = -0.29$; $p = 0.039$) and 5-sulfoxymethylfurfural ($r = -0.39$; $p = 0.003$).

Discussion

This report is the first to describe a metabolomic study in NC-AME patients. The study was based on an untargeted metabolomic analysis of serum samples from NC-AME patients and identified 36 differentially regulated metabolites, specifically 3 upregulated metabolites and 33 downregulated metabolites. For these 36 metabolites, we evaluated their diagnostic capacity as biomarkers for this phenotype.

We observed that L-dopachrome and SPMA had the highest sensitivity and specificity to discriminate the NC-AME condition, followed by bilirubin, L-iditol, deoxyribose 1-phosphate, citric acid, gamma-L-glutamyl-L-methionine sulfoxide and 5-sulfoxymethylfurfural. However, correlation analyses adjusted by age, BMI, SBP and DBP showed significant association of gamma-L-glutamyl-L-methionine sulfoxide and SMF with cortisone, which is one of the primary characteristics of this phenotype. These metabolites and their respective metabolic pathways should help to identified etiopathogenesis associated to the NC-AME condition.

In this sense, gamma-L-glutamyl-L-methionine sulfoxide, L-dopachrome and SMF were significantly increased in NC-AME patients (Table 2; Figure 4). The gamma-L-glutamyl-L-methionine is an organic compound that belongs to the class of dipeptides and is generated in conditions of oxidative stress [29,30]. Methionine sulfoxide has been proposed as a physiological marker of oxidative stress, which is a key mechanism of endothelial dysfunction, as observed in NC-AME subjects and even more notably in hypertensive patients [31]. In keeping with these data, Zhao and colleagues in a

urine metabolomic study revealed the involvement of oxidative stress metabolic pathways and amino acid metabolism in essential hypertension [32]. Moreover, early research suggested that essential hypertensives (EH) may be a disorder of inherited amino acid metabolism [33]. However, the increased levels of these two metabolites have rarely been explored in NC-AME. Similarly, L-dopachrome belongs to the class of organic compounds known as l-alpha-amino acids, and elevated levels of this metabolite indicate an increase in tyrosine metabolism, which includes the biosynthesis of melanin [34,35]. In this way, gamma-L-glutamyl-L-methionine, L-dopachrome or metabolites associated with this metabolic pathway should be further evaluated as endogenous inhibitors of 11β-HSD2, and further research is required to reveal such effects.

Along with the findings described above, we also observed that the subjects with NC-AME have high levels of the organic compound SMF, which is also negatively associated with serum cortisone. SMF comes from the metabolism of 5-hydroxymethylfurfural, a reactive metabolite that can bind to DNA and cause mutagenic effects [36]. SMF is toxic, since it accumulates in kidney proximal tubules by improper excretion due to renal reabsorption processes [37], which leads to the abovementioned damage to DNA and proteins. In addition, we show that SPMA has a good diagnostic ability to identify this phenotype of NC-AME. SPMA belongs to the family of N-acyl-alpha amino acids and derivatives and is a benzene metabolite that is catalyzed by glutathione S-transferases and has been considered a biomarker of oxidative damage. These findings may support the use of biomarkers associated with oxidative stress and renal damage, such as microalbuminuria, in NC-AME subjects.

On the other hand, bilirubin also has a good discriminatory capacity to identify the NC-AME phenotype and is decreased in these subjects. Bilirubin has previously been characterized as an antioxidative and anti-inflammatory protective factor with respect to peripheral vascular diseases [38,39], suggesting that NC-AME subjects with lower bilirubin levels may have lower protective antioxidant effects. Although various studies have shown some association of high bilirubin with a low incidence of hypertension, the present findings should be viewed with caution and should be further evaluated [40].

Other metabolites that are decreased, such as L-iditol and deoxyribose 1-phosphate, also have a good discriminatory capacity to identify the NC-AME phenotype. L-Iditol is a sugar alcohol and is part of various metabolic reactions in organisms that include fructose and mannose metabolism. On the other hand, deoxyribose 1-phosphate is involved in pentose phosphate pathways (PPPs). PPP is a multienzyme pathway that shares a common starting molecule with glycolysis, glucose-6-phosphate. PPP plays a critical role in regulating cell growth by supplying cells with not only ribose-5-phosphate but also NADPH for detoxification of intracellular ROS, reductive biosynthesis, and ribose biogenesis. Thus, the PPP can adapt to the needs of a particular cell at a time point when a change in the metabolism of a cell is required. However, these mechanisms may be affected in subjects with NC-AME.

In this report, we found low levels of citric acid in NC-AME subjects. The citric acid cycle (CAC) provides precursors of certain amino acids, as well as the reducing agent NADH, that are used in numerous reactions. Regarding 11β-HSD2 enzymatic activity, it is known that this enzyme is highly dependent on cofactor NAD^+ [6], which is essential for proper cortisol catabolic activity in the kidney and other nonepithelial tissues. Thus, a decrease in the activity of the citric acid cycle should affect the synthesis of NAD+, which is a critical cofactor for the 11β-HSD2 enzyme. The diminished CAC activity may be due to a reduction in overall mitochondrial biogenesis, reduced expression of the genes encoding citric acid enzymes, or reduced citric acid cycle substrate availability.

We observed a decrease in *S*-adenosyl-l-homocysteine (SAH), which is the metabolic precursor of homocysteine and is a negative regulator of most cell methyltransferases associated with DNA hypermethylation [41]**.** Low SAH levels observed in NC-AME subjects are indicated to be associated with higher expression of DNA-methyltransferase and

hypermethylation of the HSD11B2 promoter [42], which is expected to decrease HSD1B2 expression and subsequently affect cortisol to cortisone metabolism in these subjects. Recently, Lana et al., in a similar untargeted metabolomics analysis, EH [43], also detected a dysregulation in the urine levels of sulfur-containing metabolites (thiocysteine and homomethionine), purines (SAH, AMP, allantoate, and hydroxyisourate) and pyrimidines (dihydrothymine, uracil, and UDP), among others [43], suggesting that NC-AME may be associated with impaired sulfur-containing metabolites, such as SAH.

Finally, various publications [17,20] have addressed the effects of the inhibition of 11β-HSD2 by endogenous and exogenous inhibitors. In this study, we identified the presence of some of these endogenous inhibitors, such as cholic acid derivatives, and exogenous inhibitors, such as perfluorohexane sulfonic acid, perfluorooctanesulfonic acid, perfluorooctanoic acid, diethyl-phthalic acid, and monoethyl phthalate. However, we did not observe significant differences between the subjects with NC-AME and the healthy controls (data not shown).

In summary, the present study, based on an untargeted metabolomic assay of serum from NC-AME subjects compared with control subjects, identified a novel differential metabolite profile, observing eight perturbed metabolites L-dopachrome, S-phenylmercapturic acid, bilirubin, L-iditol, deoxyribose 1-phosphate, citric acid, gamma-L-glutamyl-L-methionine sulfoxide and 5-sulfoxymethylfurfural which are able to discriminate the NC-AME condition, highlighting gamma-L-glutamyl-L-methionine sulfoxide and 5-sulfoxymethylfurfural, that also correlate with lower cortisone concentration. These novel potential biomarkers and metabolic pathways are useful for the design of novel algorithms associated with the NC-AME phenotype. However, the pathophysiological mechanism governing this condition have not been elucidated, and *in vitro* assays are needed to define the roles of some metabolites in 11β-HSD2 expression and activity and to prove the applicability of metabolic profiling to improve the diagnosis of NC-AME subjects.

Declarations

Declaration of interest.

The authors declare that there is no conflict of interest that could be perceived as prejudicing the impartiality of this review.

Acknowledgments.

We acknowledge all the patients and researchers who supported previous studies associated with this manuscript.

Funding statements.

This study was supported by the following grants: CONICYT-FONDECYT 1150437, 1160695, and 1160836; FONDECYT POSTDOCTORAL 3200646; CONICYT-FONDEQUIP EQM150023; ANID – Millennium Science Initiative Program- IMII P09/016-F, ICN09_016; CORFO BMRC-13CTI-21526-P1; and CETREN-UC.

Authors' contributions

A.T-C. designed the study, collected, analyzed and interpreted the patient data, analyzed the metabolomics data, wrote the first draft of the manuscript, contributed to discussion, and reviewed the manuscript. CA.C. collected and analyzed data, contributed to the statistics of the data, contributed to discussion and reviewed the manuscript. A.V. contributed to

discussion and reviewed the manuscript. CE.F enrolled patients, analyzed and interpreted the patient data, contributed to discussion, and reviewed the manuscript. All authors approved the final version.

References

1. Yau, M. *et al.* Clinical, genetic, and structural basis of apparent mineralocorticoid excess due to 11beta-hydroxysteroid dehydrogenase type 2 deficiency. *Proc Natl Acad Sci U S A***114**, E11248-E11256, doi:10.1073/pnas.1716621115 (2017).
2. Arriza, J. L. *et al.* Cloning of human mineralocorticoid receptor complementary DNA: structural and functional kinship with the glucocorticoid receptor. *Science***237**, 268-275 (1987).
3. Arriza, J. L., Simerly, R. B., Swanson, L. W. & Evans, R. M. The neuronal mineralocorticoid receptor as a mediator of glucocorticoid response. *Neuron***1**, 887-900 (1988).
4. Ferrari, P., Lovati, E. & Frey, F. J. The role of the 11beta-hydroxysteroid dehydrogenase type 2 in human hypertension. *J Hypertens***18**, 241-248 (2000).
5. Carvajal, C. A., Tapia-Castillo, A., Vecchiola, A., Baudrand, R. & Fardella, C. E. Classic and Nonclassic Apparent Mineralocorticoid Excess Syndrome. *J Clin Endocrinol Metab***105**, doi:10.1210/clinem/dgz315 (2020).
6. Carvajal, C. A. *et al.* Two homozygous mutations in the 11 beta-hydroxysteroid dehydrogenase type 2 gene in a case of apparent mineralocorticoid excess. *J Clin Endocrinol Metab***88**, 2501-2507, doi:10.1210/jc.2002-021909 (2003).
7. Carvajal, C. A. *et al.* Serum Cortisol and Cortisone as Potential Biomarkers of Partial 11beta-Hydroxysteroid Dehydrogenase Type 2 Deficiency. *Am J Hypertens***31**, 910-918, doi:10.1093/ajh/hpy051 (2018).
8. Mune, T., Rogerson, F. M., Nikkila, H., Agarwal, A. K. & White, P. C. Human hypertension caused by mutations in the kidney isozyme of 11 beta-hydroxysteroid dehydrogenase. *Nat Genet***10**, 394-399, doi:10.1038/ng0895-394 (1995).
9. Tapia-Castillo, A. *et al.* Clinical, Biochemical, and Genetic Characteristics of "Nonclassic" Apparent Mineralocorticoid Excess Syndrome. *J Clin Endocrinol Metab***104**, 595-603, doi:10.1210/jc.2018-01197 (2019).
10. Baudrand, R. & Vaidya, A. The Low-Renin Hypertension Phenotype: Genetics and the Role of the Mineralocorticoid Receptor. *International journal of molecular sciences***19**, pii: E546., doi:10.3390/ijms19020546 (2018).
11. Baudrand, R. *et al.* Continuum of Renin-Independent Aldosteronism in Normotension. *Hypertension***69**, 950-956, doi:10.1161/HYPERTENSIONAHA.116.08952 (2017).
12. Brown, J. M. *et al.* The Spectrum of Subclinical Primary Aldosteronism and Incident Hypertension: A Cohort Study. *Ann Intern Med***167**, 630-641, doi:10.7326/M17-0882 (2017).
13. Tapia-Castillo, A. *et al.* Downregulation of exosomal miR-192-5p and miR-204-5p in subjects with nonclassic apparent mineralocorticoid excess. *Journal of translational medicine***17**, 392, doi:10.1186/s12967-019-02143-8 (2019).
14. Morris, D. J. *et al.* Detection of glycyrrhetinic acid-like factors (GALFs) in human urine. *Hypertension***20**, 356-360, doi:10.1161/01.hyp.20.3.356 (1992).
15. Morris, D. J., Latif, S. A., Hardy, M. P. & Brem, A. S. Endogenous inhibitors (GALFs) of 11beta-hydroxysteroid dehydrogenase isoforms 1 and 2: derivatives of adrenally produced corticosterone and cortisol. *J Steroid Biochem Mol Biol***104**, 161-168, doi:10.1016/j.jsbmb.2007.03.020 (2007).
16. Latif, S. A., Sheff, M. F., Ribeiro, C. E. & Morris, D. J. Selective inhibition of sheep kidney 11 beta-hydroxysteroid dehydrogenase isoform 2 activity by 5 alpha-reduced (but not 5 beta) derivatives of adrenocorticosteroids. *Steroids***62**, 230-237 (1997).

17. Ma, X., Lian, Q. Q., Dong, Q. & Ge, R. S. Environmental inhibitors of 11beta-hydroxysteroid dehydrogenase type 2. *Toxicology***285**, 83-89, doi:10.1016/j.tox.2011.04.007 (2011).
18. Latif, S. A., Conca, T. J. & Morris, D. J. The effects of the licorice derivative, glycyrrhetinic acid, on hepatic 3 alpha- and 3 beta-hydroxysteroid dehydrogenases and 5 alpha- and 5 beta-reductase pathways of metabolism of aldosterone in male rats. *Steroids***55**, 52-58 (1990).
19. Kumagai, A., Yano, S. & Otomo, M. Study on the corticoid-like action of glycyrrhizine and the mechanism of its action. *Endocrinologia japonica***4**, 17-27 (1957).
20. Zhou, C., Ye, F., Wu, H., Ye, H. & Chen, Q. Recent advances in the study of 11beta-Hydroxysteroid dehydrogenase type 2 (11beta-HSD2)Inhibitors. *Environmental toxicology and pharmacology***52**, 47-53, doi:10.1016/j.etap.2017.02.021 (2017).
21. Patti, G. J., Yanes, O. & Siuzdak, G. Innovation: Metabolomics: the apogee of the omics trilogy. *Nature reviews. Molecular cell biology***13**, 263-269, doi:10.1038/nrm3314 (2012).
22. Wawrzyniak, R. *et al.* Untargeted Metabolomics Provides Insight into the Mechanisms Underlying Resistant Hypertension. *Current medicinal chemistry***26**, 232-243, doi:10.2174/0929867324666171006122656 (2019).
23. Mulatero, P. *et al.* Drug effects on aldosterone/plasma renin activity ratio in primary aldosteronism. *Hypertension***40**, 897-902 (2002).
24. Montero, J., Soto, J., Fardella, C., Foradori, A. & Valdes, G. [Measurement of low levels of plasma renin activity. A methodological improvement]. *Rev Med Chil***126**, 151-154 (1998).
25. Whelton, P. K. *et al.* 2017 ACC/AHA/AAPA/ABC/ACPM/AGS/APhA/ASH/ASPC/NMA/PCNA Guideline for the Prevention, Detection, Evaluation, and Management of High Blood Pressure in Adults: A Report of the American College of Cardiology/American Heart Association Task Force on Clinical Practice Guidelines. *J Am Coll Cardiol***71**, 1269-1324, doi:10.1016/j.jacc.2017.11.006 (2017).
26. Liu, X. *et al.* Discovery and validation of plasma biomarkers for major depressive disorder classification based on liquid chromatography-mass spectrometry. *Journal of proteome research***14**, 2322-2330, doi:10.1021/acs.jproteome.5b00144 (2015).
27. Chen, C. *et al.* Metabolomics reveals metabolite changes of patients with pulmonary arterial hypertension in China. *J Cell Mol Med***24**, 2484-2496, doi:10.1111/jcmm.14937 (2020).
28. Zhao, J. H. *et al.* Circulating Plasma Metabolomic Profiles Differentiate Rodent Models of Pulmonary Hypertension and Idiopathic Pulmonary Arterial Hypertension Patients. *Am J Hypertens***32**, 1109-1117, doi:10.1093/ajh/hpz121 (2019).
29. Cabreiro, F., Picot, C. R., Friguet, B. & Petropoulos, I. Methionine sulfoxide reductases: relevance to aging and protection against oxidative stress. *Annals of the New York Academy of Sciences***1067**, 37-44, doi:10.1196/annals.1354.006 (2006).
30. Picot, C. R. *et al.* Alterations in mitochondrial and cytosolic methionine sulfoxide reductase activity during cardiac ischemia and reperfusion. *Experimental gerontology***41**, 663-667, doi:10.1016/j.exger.2006.03.011 (2006).
31. Guzik, T. J. & Touyz, R. M. Oxidative Stress, Inflammation, and Vascular Aging in Hypertension. *Hypertension***70**, 660-667, doi:10.1161/HYPERTENSIONAHA.117.07802 (2017).
32. Zhao, H. *et al.* Identification of essential hypertension biomarkers in human urine by non-targeted metabolomics based on UPLC-Q-TOF/MS. *Clinica chimica acta; international journal of clinical chemistry***486**, 192-198, doi:10.1016/j.cca.2018.08.006 (2018).
33. Min, X., Lee, B. H., Cobb, M. H. & Goldsmith, E. J. Crystal structure of the kinase domain of WNK1, a kinase that causes a hereditary form of hypertension. *Structure***12**, 1303-1311, doi:10.1016/j.str.2004.04.014 (2004).

34. Tsukamoto, K., Jackson, I. J., Urabe, K., Montague, P. M. & Hearing, V. J. A second tyrosinase-related protein, TRP-2, is a melanogenic enzyme termed DOPAchrome tautomerase. *The EMBO journal***11**, 519-526 (1992).
35. Leonard, L. J., Townsend, D. & King, R. A. Function of dopachrome oxidoreductase and metal ions in dopachrome conversion in the eumelanin pathway. *Biochemistry***27**, 6156-6159, doi:10.1021/bi00416a049 (1988).
36. Monien, B. H., Engst, W., Barknowitz, G., Seidel, A. & Glatt, H. Mutagenicity of 5-hydroxymethylfurfural in V79 cells expressing human SULT1A1: identification and mass spectrometric quantification of DNA adducts formed. *Chemical research in toxicology***25**, 1484-1492, doi:10.1021/tx300150n (2012).
37. Bakhiya, N., Monien, B., Frank, H., Seidel, A. & Glatt, H. Renal organic anion transporters OAT1 and OAT3 mediate the cellular accumulation of 5-sulfooxymethylfurfural, a reactive, nephrotoxic metabolite of the Maillard product 5-hydroxymethylfurfural. *Biochemical pharmacology***78**, 414-419, doi:10.1016/j.bcp.2009.04.017 (2009).
38. Djousse, L. *et al.* Total serum bilirubin and risk of cardiovascular disease in the Framingham offspring study. *The American journal of cardiology***87**, 1196-1200; A1194, 1197, doi:10.1016/s0002-9149(01)01494-1 (2001).
39. Kunutsor, S. K., Bakker, S. J., Gansevoort, R. T., Chowdhury, R. & Dullaart, R. P. Circulating total bilirubin and risk of incident cardiovascular disease in the general population. *Arteriosclerosis, thrombosis, and vascular biology***35**, 716-724, doi:10.1161/ATVBAHA.114.304929 (2015).
40. Chin, H. J. *et al.* The bilirubin level is negatively correlated with the incidence of hypertension in normotensive Korean population. *Journal of Korean medical science***24 Suppl**, S50-56, doi:10.3346/jkms.2009.24.S1.S50 (2009).
41. James, S. J., Melnyk, S., Pogribna, M., Pogribny, I. P. & Caudill, M. A. Elevation in S-adenosylhomocysteine and DNA hypomethylation: potential epigenetic mechanism for homocysteine-related pathology. *The Journal of nutrition***132**, 2361S-2366S, doi:10.1093/jn/132.8.2361S (2002).
42. Pizzolo, F. *et al.* Apparent Mineralocorticoid Excess by a Novel Mutation and Epigenetic Modulation by HSD11B2 Promoter Methylation. *J Clin Endocrinol Metab***100**, E1234-1241, doi:10.1210/jc.2015-1760 (2015).
43. Lana, A. *et al.* Urinary Metabolic Signature of Primary Aldosteronism: Gender and Subtype-Specific Alterations. *Proteomics. Clinical applications***13**, e1800049, doi:10.1002/prca.201800049 (2019).

Figures

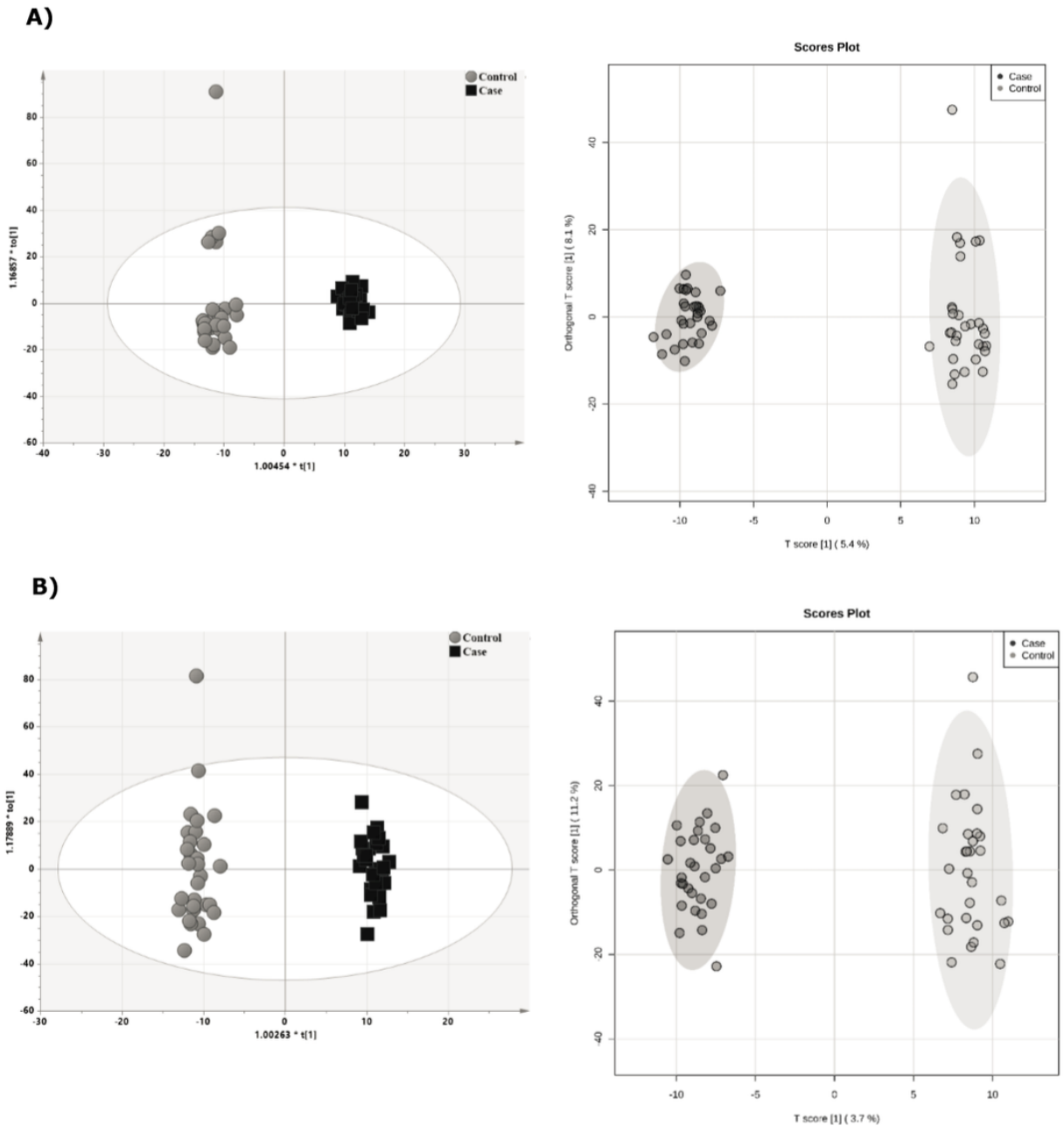

Figure 1

Discriminant analysis of groups. A) Scores scatter plot of OPLS-DA model of samples run in negative ion mode B) Scores scatter plot of OPLS-DA model of samples run in positive ion mode.

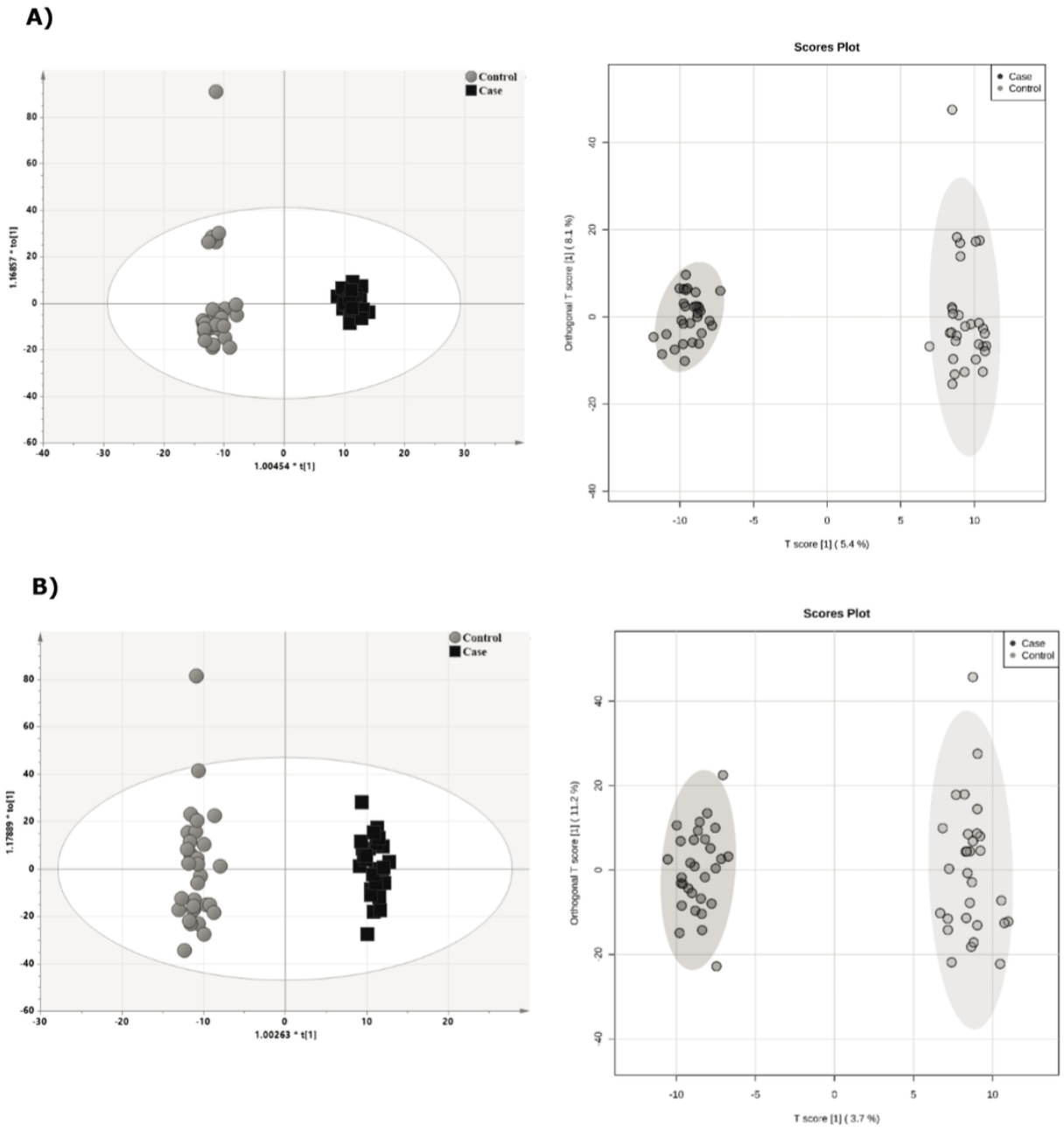

Figure 1

Discriminant analysis of groups. A) Scores scatter plot of OPLS-DA model of samples run in negative ion mode B) Scores scatter plot of OPLS-DA model of samples run in positive ion mode.

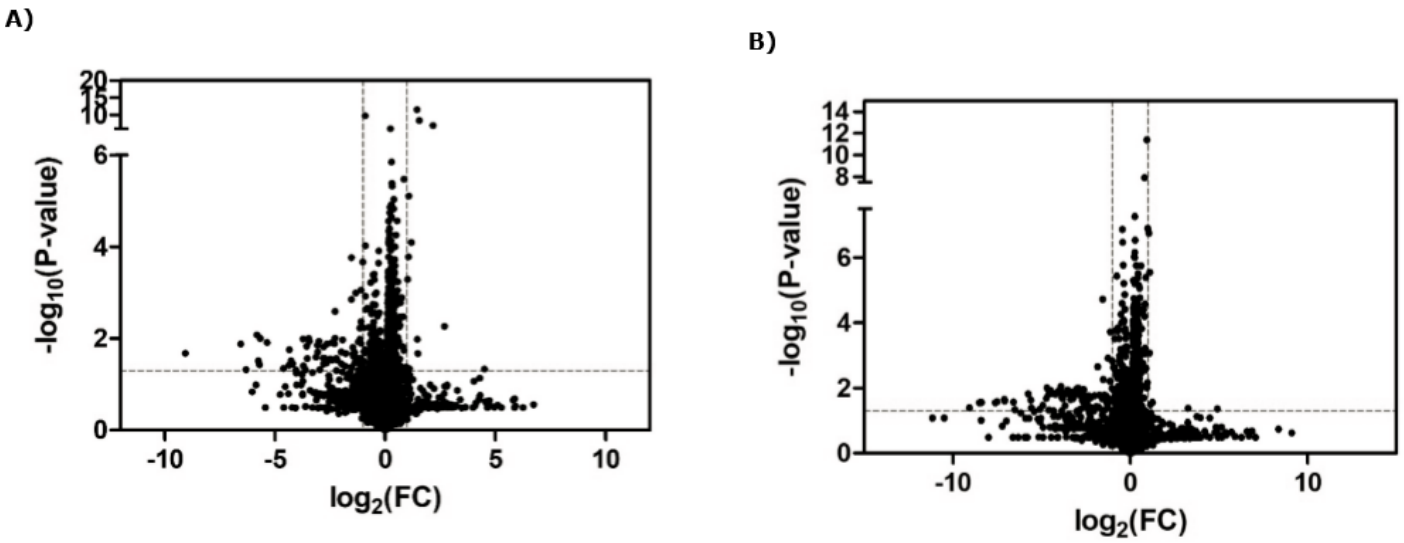

Figure 2

Volcano plot of differential abundance of metabolites found in metabolomics assay of NC-AME versus control subjects. The X-axis is the Log2 of metabolites levels (fold change) between subjects with NC-AME and control subjects. The Y-axis adjusts the p value as a function of -Log10. The range of Y>1.30 and X>1 were significant increase; The range of Y>1.30 and X<1 were significant decrease. A) At negative ion mode B) At positive ion mode.

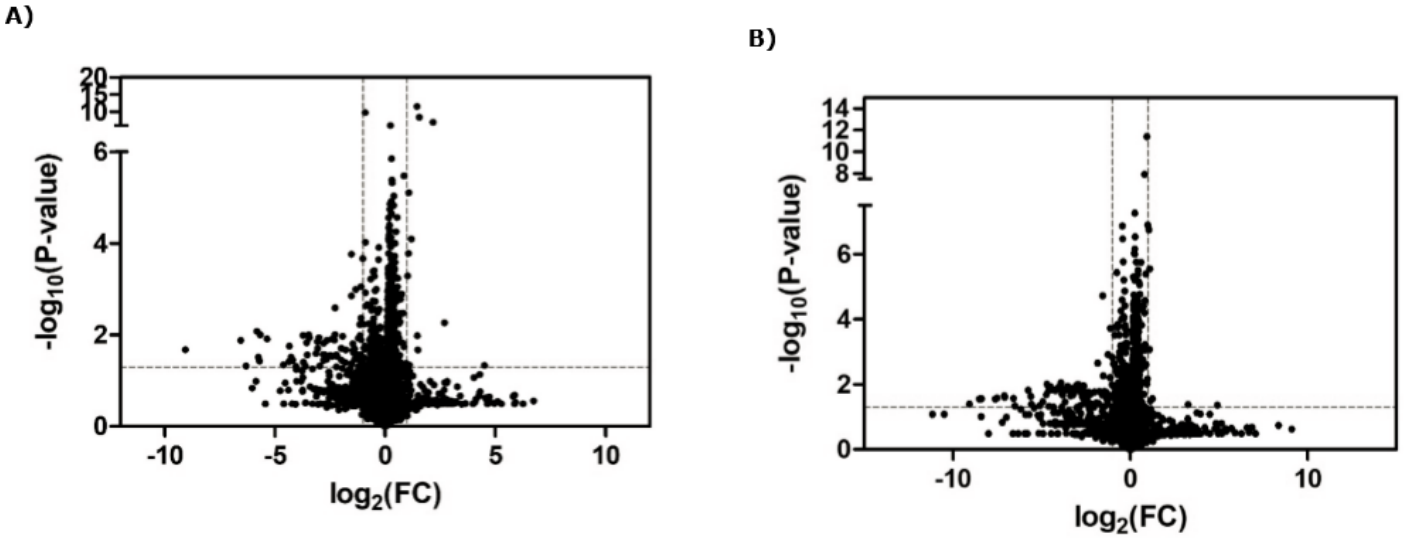

Figure 2

Volcano plot of differential abundance of metabolites found in metabolomics assay of NC-AME versus control subjects. The X-axis is the Log2 of metabolites levels (fold change) between subjects with NC-AME and control subjects. The Y-axis adjusts the p value as a function of -Log10. The range of Y>1.30 and X>1 were significant increase; The range of Y>1.30 and X<1 were significant decrease. A) At negative ion mode B) At positive ion mode.

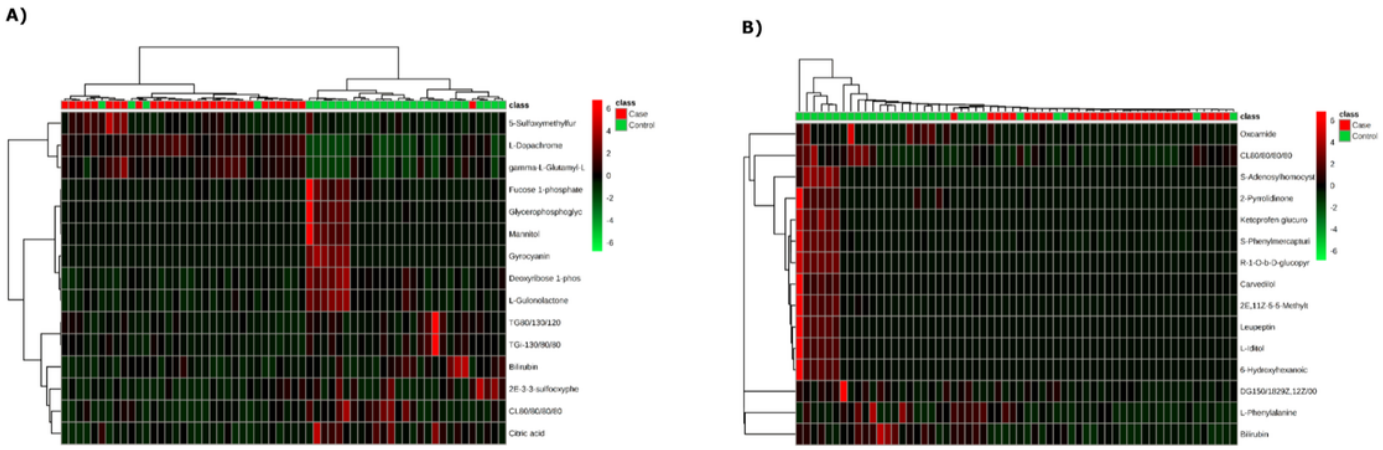

Figure 3

Hierarchical cluster analysis of metabolome data from significant metabolites. A) At negative ion mode B) At positive ion mode.

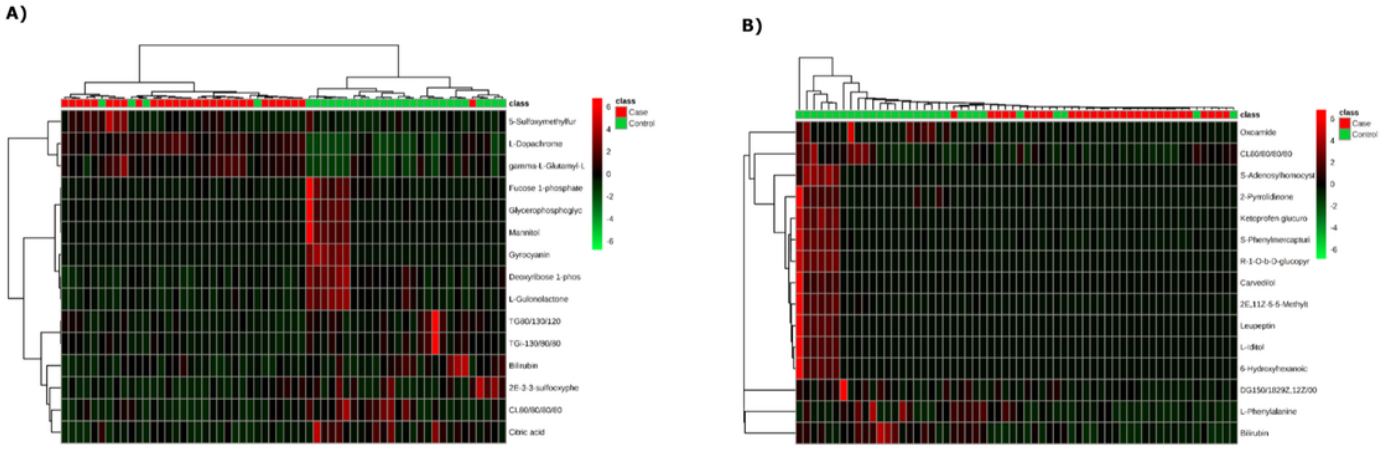

Figure 3

Hierarchical cluster analysis of metabolome data from significant metabolites. A) At negative ion mode B) At positive ion mode.

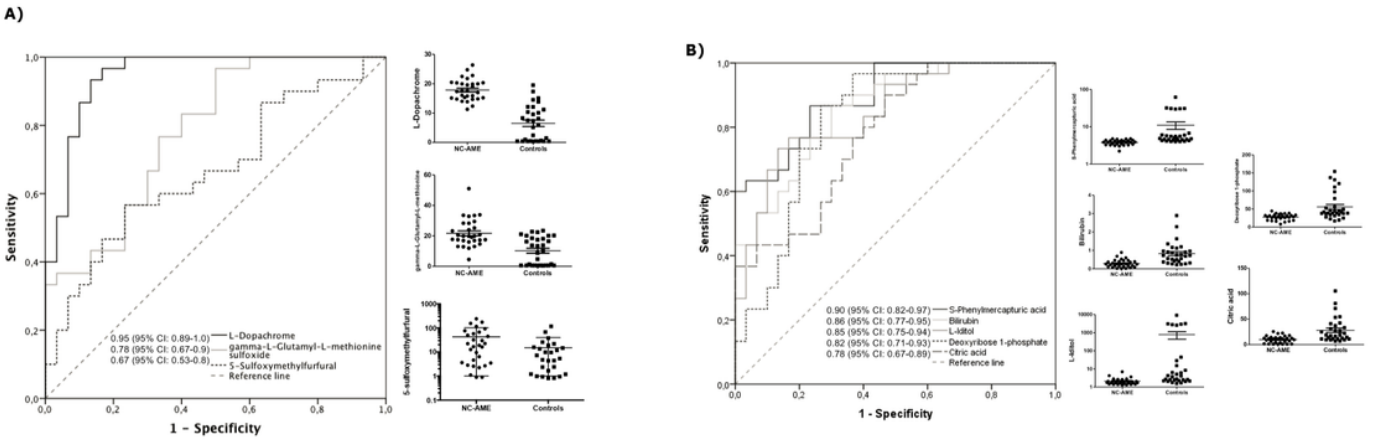

Figure 4

Evaluation of diagnostic efficacy using ROC curve for top 8 metabolites in serum differentially expressed in NC-AME and control subjects, as detected by UPLC-TOF-MS. A) Upregulated metabolites; B) Downregulated metabolites.

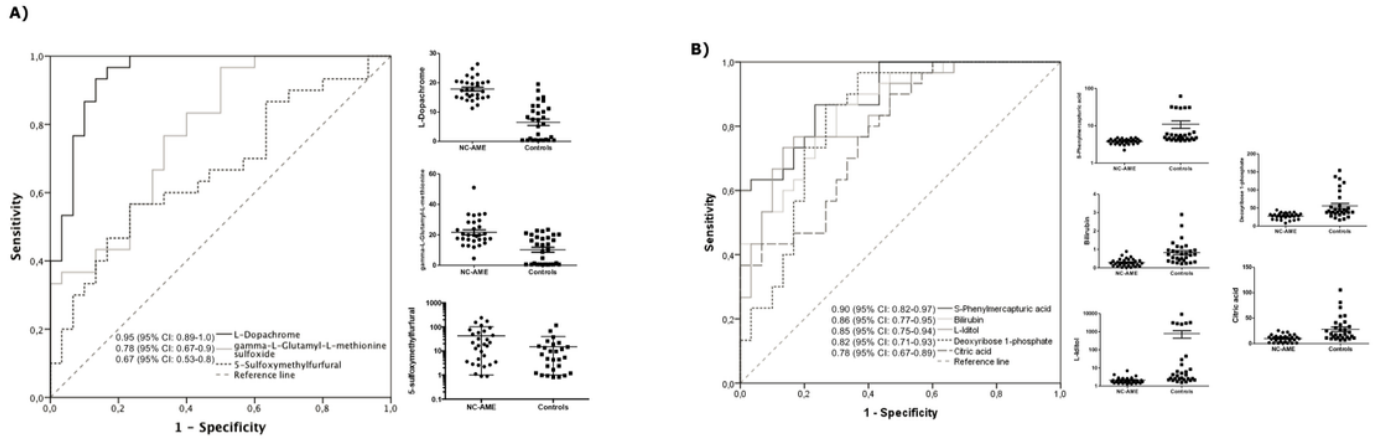

Figure 4

Evaluation of diagnostic efficacy using ROC curve for top 8 metabolites in serum differentially expressed in NC-AME and control subjects, as detected by UPLC-TOF-MS. A) Upregulated metabolites; B) Downregulated metabolites.

Supplementary Files

This is a list of supplementary files associated with this preprint. Click to download.

- TapiaCastilloSuppldataScientificReports.pdf
- TapiaCastilloSuppldataScientificReports.pdf